भारतीय मानक

Indian Standard

IS 16413 : 2023
ISO/TS 10867 : 2019

नैनोप्रौद्योगिकी — अवरक्त फोटोलुमिनियस स्पेक्ट्रोस्कोपी के समीपस्थ के प्रयोग से सिंगल-वॉल कार्बन नैनो ट्यूबों के अभिलक्षण

(पहला पुनरीक्षण)

Nanotechnologies — Characterization of Single-Wall Carbon Nanotubes Using Near Infrared Photoluminescence Spectroscopy

(First Revision)

ICS 07.120

भारतीय मानक ब्यूरो
BUREAU OF INDIAN STANDARDS
मानक भवन, 9 बहादुर शाह ज़फर मार्ग, नई दिल्ली - 110002
MANAK BHAVAN, 9 BAHADUR SHAH ZAFAR MARG
NEW DELHI - 110002
www.bis.gov.in www.standardsbis.in

August 2023 **Price Group 9**

Nanotechnologies Sectional Committee, MTD 33

NATIONAL FOREWORD

This Indian Standard (First Revision) which is identical to ISO/TS 10867 : 2019 ‘Nanotechnologies — Characterization of single-wall carbon nanotubes using near infrared photoluminescence spectroscopy’ issued by the International Organization for Standardization (ISO) was adopted by the Bureau of Indian Standards on the recommendation of the Nanotechnologies Sectional Committee and approval of the Metallurgical Engineering Division Council.

This standard was originally published in 2017 by adoption of ISO/TS 10867 : 2010. The first revision of this standard has been undertaken to align with the latest version ISO/TS 10867 : 2019 which has been technically revised.

The text of ISO standard has been approved as suitable for publication as in Indian Standard without deviations. Certain terminologies and conventions are, however, not identical with those used in Indian Standard. Attention is especially drawn to the following:

a) Wherever the words ‘International Standard’ appear referring to this standard, it should be read as ‘Indian Standard’; and
b) Comma (,) has been used as a decimal marker while in Indian Standards the current practice is to use a point (.) as the decimal marker.

In this adopted standard, reference appears to certain International Standards for which Indian Standards also exist. The corresponding Indian Standards which are to be substituted in their place are listed below along with their degree of equivalence for the edition indicated:

International Standard	*Corresponding Indian Standard*	*Degree of Equivalence*
ISO/TS 80004-4 : 2011 Nanotechnologies — Vocabulary — Part 4: Nanostructured materials	IS/ISO 80004-4 : 2011 Nanotechnologies — Vocabulary: Part 4 Nanostructured materials	Identical
ISO/TS 80004-6 : 2021 Nanotechnologies — Vocabulary — Part 6: Nano-object characterization	IS 17003 (Part 6) : 2018/ISO 80004-6 : 2013 Nanotechnologies — Vocabulary: Part 6 Nano-object characterization	Identical

In reporting the result of a test or analysis made in accordance with this standard, is to be rounded off, it shall be done in accordance with IS 2 : 2022 ‘Rules for rounding off numerical values (*second revision*)’.

Contents

Page

Introduction

The discovery of the band-gap photoluminescence (PL) of single-wall carbon nanotubes (SWCNTs) has provided a useful method to characterize their unique electronic properties induced by their low-dimensionality. This method is described in this document.

Indian Standard

NANOTECHNOLOGIES — CHARACTERIZATION OF SINGLE-WALL CARBON NANOTUBES USING NEAR INFRARED PHOTOLUMINESCENCE SPECTROSCOPY

(First Revision)

1 Scope

This document gives guidelines for the characterization of single-wall carbon nanotubes (SWCNTs) using near infrared (NIR) photoluminescence (PL) spectroscopy.

It provides a measurement method for the determination of the chiral indices of the semi-conducting SWCNTs in a sample and their relative integrated PL intensities.

The method can be expanded to estimate the relative mass concentrations of semi-conducting SWCNTs in a sample from their measured integrated PL intensities and knowledge of their PL cross-sections.

2 Normative references

The following documents are referred to in the text in such a way that some or all of their content constitutes requirements of this document. For dated references, only the edition cited applies. For undated references, the latest edition of the referenced document (including any amendments) applies.

ISO/TS 80004-4, *Nanotechnologies — Vocabulary — Part 4: Nanostructured materials*

ISO/TS 80004-6, *Nanotechnologies — Vocabulary — Part 6: Nano-object characterization*

3 Terms and definitions

For the purposes of this document, the terms and definitions given in ISO/TS 80004-4, ISO/TS 80004-6 and the following apply.

ISO and IEC maintain terminological databases for use in standardization at the following addresses:

— ISO Online browsing platform: available at https://www.iso.org/obp

— IEC Electropedia: available at http://www.electropedia.org/

3.1
chirality
vector notation used to describe the structure of a single-wall carbon nanotube (SWCNT)

3.2
chiral indices
two integers that define the chiral vector of a single-wall carbon nanotube (SWCNT)

3.3
relative mass concentration
mass concentration of a nanotube species relative to that of the most common nanotube species

4 Principles of band gap photoluminescence of SWCNTs

4.1 Structure of SWCNTs

A SWCNT consists of a single cylindrical graphene layer. The specific geometry of SWCNTs is defined in terms of a chiral vector containing a length (the tube's circumference) and a chiral angle α (ranging from 0° to 30°). Alternatively, the structure of SWCNTs is defined by the chiral indices (n, m). Figure 1 shows the indexed graphene sheet with chiral vector for designating the nanotube structure, and how the vector starting at point (0,0) to (n, m) determines the nanotube designation[1]. The chiral angle is measured between the zigzag structure (α = 0°) and the chiral vector. When the chiral angle is between 0° and 30°, a chiral structure arises. The SWCNT that has the maximum chiral angle, 30°, is called the armchair SWCNT.

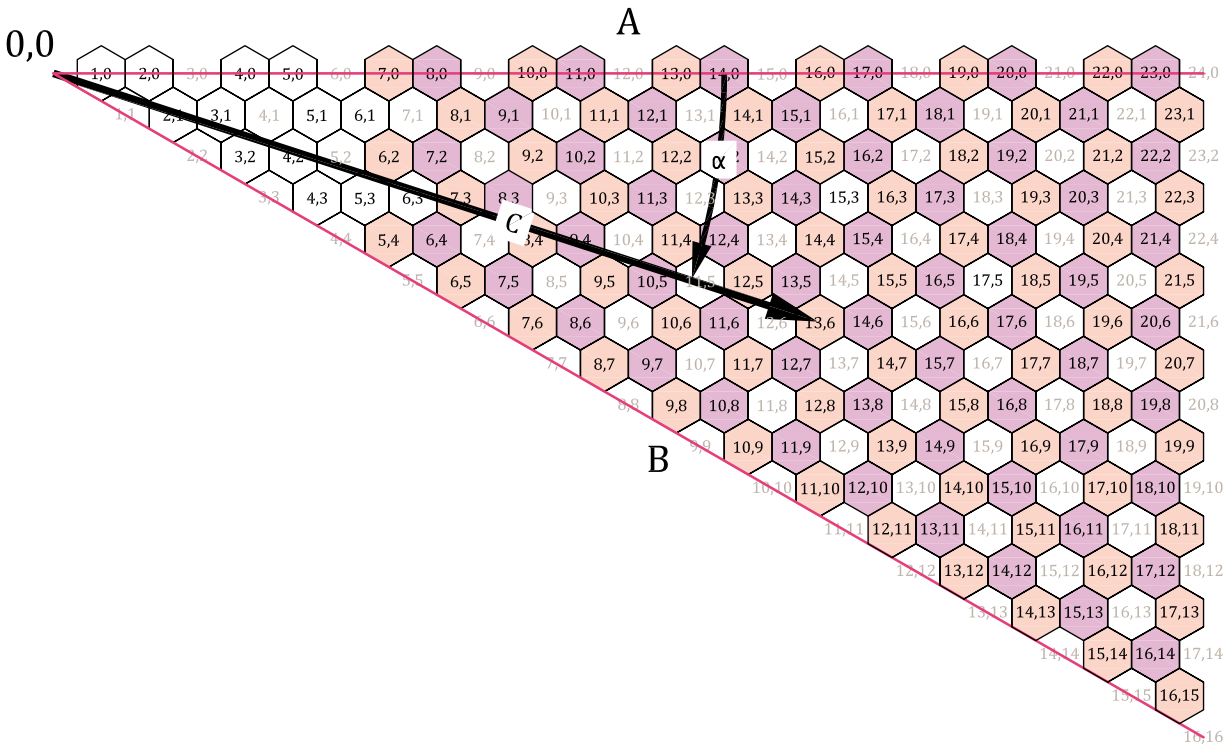

Key

A zigzag structure

B armchair structure

C chiral vector

NOTE The chiral angle α and chiral vector are shown. The grey indices are for nanotubes that are not photoluminescent.

Figure 1 — Indexed graphene sheet with chiral vector for designating nanotube structure

The length of the chiral vector is the circumference of the tube, or π × the tube diameter d_t. The tube diameter d_t is given in terms of (n, m) as shown by Formula (1):

$$d_t = L/\pi = \frac{\sqrt{3}a_{C-C}\sqrt{m^2+mn+n^2}}{\pi} \quad (1)$$

where

d_t is the diameter of the SWCNT;

L is the length of the chiral vector;

a_{C-C} is the nearest-neighbour distance (0,144 nm) between pairs of carbon atoms;

m is one of the chiral indices;

n is the other chiral index.

The chiral angle α in terms of (n, m) is defined as shown by Formula (2):

$$\alpha = \tan^{-1}\left[\sqrt{3}m/(2n+m)\right] \quad (2)$$

where

α is the chiral angle;

m is one of the chiral indices;

n is the other chiral index.

4.2 Band structure and PL peaks

Quasi-one-dimensional SWCNTs have an electronic density of states roughly as shown in Figure 2, with sharp van Hove peaks such as v_1 and v_2 (in the valence band) and c_1 and c_2 (in the conduction band).

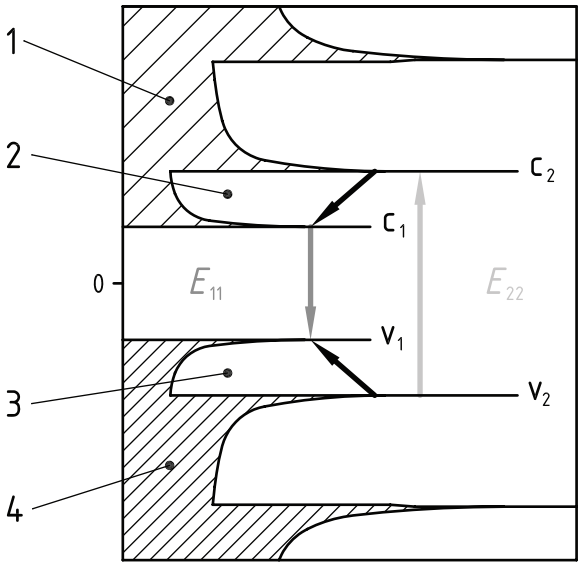

Key

1 conduction band
2 non-radiative relaxation of electron
3 non-radiative relaxation of hole
4 valence band

Figure 2 — Qualitative description of the electronic density of states for SWCNTs[2]

Just as the positions of the van Hove peaks depend on the structure (and chiral vector) of the particular SWCNTs, so will the absorption energy E_{22} and fluorescent emission energy E_{11}. Therefore, the positions of the spectral peaks corresponding to E_{22} and E_{11} are characteristic of the structure of each SWCNT

and can be used as a measurement method to determine the component SWCNTs of an unknown mixture. Formula (3) relates peak wavelength to transition energy:

$$E = hc/\lambda = hc\bar{\nu} \tag{3}$$

where

E is energy of the transition;

c is the speed of light;

h is Planck's constant;

$\bar{\nu}$ is the peak position, expressed in wavenumber units (cm^{-1});

λ is the wavelength of the photon absorbed or emitted.

Those structures where the difference ($n - m$) is divisible by three [e.g. (3,0), (4,1) or (6,3)], and those structures where $n = m$, do not fluoresce because SWCNTs with ($n - m$) = a multiple of three are quasi-metals, with a band gap in the meV range, and those with $n = m$ are metals (no band gap). The remaining structures are semi-conductors with a band gap of about 0,5 eV to 1 eV [1 eV = 1,602 176 53 (14) × 10^{-19} J] and can fluoresce under specific sample preparation conditions.

NOTE As-prepared SWCNT samples contain left- and right-handed helical structures. The intrinsic peak positions of the PL signals are basically the same for these enantiomers although they can be affected differently by absorbates. Also, their cross-sections with respect to polarized light can differ.

4.3 Exciton effects

Electron-hole pair excitations giving rise to PL are better described in terms of excitons. Excitons are the result of Coulomb interaction, which for SWCNTs is very important and significantly affects the energy spectrum (e.g. with phonon sidebands and excitonic manifolds of excited states) and the strength of optical transitions. The exciton binding energy was estimated to be 0,420 eV for SWCNTs with a diameter of 0,8 nm in a polymer matrix and a surfactant solution[3]. This value substantially depends on the nanotube environment. An exciton band structure is shown in Figure 3.

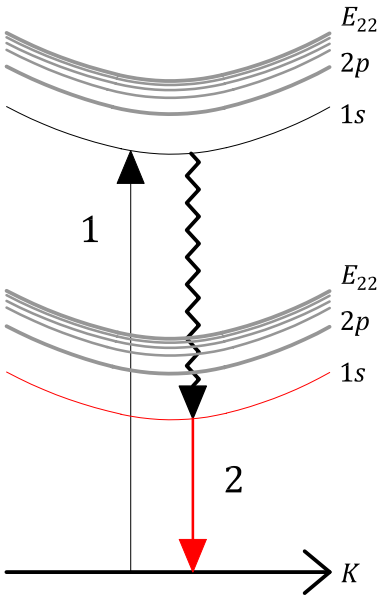

Key

1 absorption

2 emission

Figure 3 — Qualitative description of the exciton band structure of SWCNTs

5 NIR-PL apparatus

5.1 NIR-PL spectrometer

For SWCNTs produced by the chemical vapor deposition (CVD) method with a typical diameter distribution of 0,6 nm to 1,3 nm, a NIR detector covering the spectral range from 800 nm to 1 600 nm is sufficient to detect their PL. However, to detect the PL signal of a larger diameter SWCNT produced by laser vaporization and electric arc techniques, a spectral range of 1 200 nm to 2 000 nm is usually required.

NOTE 1 Examples of detector materials are InGaAs and InP/InGaAs.

NOTE 2 The spectral resolution, which in a scanning monochrometer is a complex function of the bandpass of the monochromators, the stepping increment and slit width, needs to be adjusted to resolve the SWCNT peaks of interest in the sample. In general, bandpass values approaching 10 nm have been shown to be sufficient for most surfactant suspensions of SWCNTs. With multi-channel NIR detection systems, a resolution of 5 nm is recommended.

5.2 Light source

Excitation sources are available, such as monochromated Xenon or tungsten lamps, continuous Titanium-Sapphire lasers, fixed wavelength diode lasers or white light lasers.

NOTE Suitable wavelengths of diode lasers can be selected to suit the chirality distribution of the SWCNT sample (see Figure A.2 and Figure A.4).

6 Sample preparation methods

6.1 Preparation of dispersion for measurement

For the preparation of a liquid dispersion of SWCNTs, the following procedure is recommended.

a) Use D_2O as the dispersing medium, which transmits light in the broad range from UV-Vis to 1 800 nm.

NOTE 1 H_2O is unsuitable because it strongly absorbs light at 1 400 nm and longer wavelengths.

NOTE 2 Organic solvents such as toluene can also be used for dispersing medium[4][5].

b) Use water-soluble surfactants as dispersants, preferably anionic ones such as sodium deoxycholate (SDC) (purity > 96 %), sodium dodecyl sulfate (SDS) (purity > 95 %), sodium dodecylbenzene sulfonate (SDBS) (purity > 95 %) or sodium cholate (SC) (purity > 98 %).

NOTE 3 Recent work suggests using sodium deoxycholate (SDC) over other dispersants[6].

NOTE 4 For biological applications, DNA and polyethylene glycol (PEG) are preferentially used as dispersants[7][8].

c) Prepare a D_2O solution of a dispersant, approximately at a concentration of 1 % mass fraction.

d) Add a small amount (approximately 1 mg) of the sample containing SWCNTs into the dispersant solution, approximately 20 ml.

e) To facilitate the process and to obtain a homogeneous SWCNT dispersion, sonicate the mixture using an ultrasonic homogenizer.

NOTE 5 An example of sonication conditions is given in Annex A.

NOTE 6 Even after the sonication steps, there can be a significant amount of bundled SWCNTs in the micelle solution.

NOTE 7 Keep the mixture temperature low by placing the container in an ice bath during sonication.

f) To separate the bundled SWCNTs from the isolated SWCNTs, ultracentrifuge the dispersion and use the supernatant for the PL measurements.

NOTE 8 An example of ultracentrifugation conditions is given in Annex A.

NOTE 9 Insufficient centrifugation leaves a large amount of the bundled SWCNTs unseparated in the sample. On the other hand, excess centrifugation causes a severe reduction in the concentration of SWCNTs in the solution.

g) If the optical density (OD) at the excitation wavelength of the probe volume is above 0,1 after sonication and centrifugation, dilute with the surfactant solution to lower the OD below 0,1.

NOTE 10 OD is per cm.

h) Adjust the pH of the solution to be approximately 8 by adding an appropriate amount of NaOH[9].

6.2 Preparation of solid film dispersion for measurement

When PL signals beyond 1 800 nm are required (e.g. when SWCNTs produced by the electric arc technique have a size larger than about 1,4 nm in diameter), prepare the sample by the following method.

a) Use H_2O as the dispersing medium to obtain the supernatant, following the same procedures as described in 6.1, including sonication and ultracentrifugation.

b) Mix the supernatant with the same volume of an H_2O solution of gelatin from an alkali-processed bovine bone with a concentration of 10 % mass fraction. Here, gelatin is used as a film-forming agent[10].

c) Cast the mixed solution onto a quartz substrate under ambient conditions and let it dry (10 h or longer). This results in the formation of an optically uniform film in which SWCNTs are homogenously dispersed.

7 Measurement procedures

The PL spectra of SWCNTs shall be measured as follows (see Figure A.1 and Figure A.3).

a) Turn on the light source, the spectrometer and the detector, and wait until they stabilize.

b) Calibrate the wavelength-dependent instrumental factors and excitation intensities. For the calibration of the PL system, it is recommended that a light source providing wavelength values traceable to the International System of Units (SI) is used for correcting the instrument's emission detector signal and a calibrated detector is used for correcting the instrument's excitation reference detector signal.

NOTE Wavelength reference values can be found in Reference [28].

c) Set the SWCNT sample in the correct position according to the spectrometer manual. For this method to work well, pre-existing knowledge is needed of SWCNT diameter ranges. The excitation wavelengths must be matched to the sample under study.

The sample cell should be transparent to the excitation and the emission wavelengths.

d) Measure the PL spectrum. Excitation wavelengths should be selected to give excitation of the range of SWCNT species to be analysed in the sample. A dense set of excitation wavelengths may be used to generate a full two-dimensional excitation-emission map, or alternatively a sparse set of excitation wavelengths may be used to generate emission spectra that can be analysed using knowledge of SWCNT peak positions[2][9][11][12][13].

e) Several different concentration solution samples should also be measured to ensure linearity and check that the sample is not damaged during the course of the measurements.

f) Compile the data to obtain a corrected excitation-emission map or a corrected set of emission spectra correlated with the excitation wavelength.

For the two-dimensional excitation-emission map, it is recommended that the units for the vertical scale are specified.

8 Data analysis and results interpretation

8.1 Empirical rules for structural assignment

To analyse spectra from numerous SWCNTs in aqueous SDS suspension, the empirical rules for relating peak position to (n, m) SWCNT structure shown in Formulae (4) and (5) apply[2][9][11]:

$$\overline{\nu_{11}} = \frac{1\times10^{7}}{157{,}5+1\,066{,}9d_{\mathrm{t}}} + \frac{A_1 \cos 3\alpha}{{d_{\mathrm{t}}}^2} \tag{4}$$

where

$\overline{\nu_{11}}$ is the emission peak position, expressed in wavenumber units (cm^{-1});

d_{t} is the diameter of SWCNTs, expressed in nanometer units (nm);

A_1 is –710 cm^{-1} and 369 cm^{-1} for (n – m) mod 3 = 1 and 2, respectively;

α is the chiral angle (°).

and

$$\overline{\nu_{22}} = \frac{1\times10^{7}}{145{,}6+575{,}7d_t} + \frac{A_2 \cos 3\alpha}{{d_t}^2} \quad (5)$$

where

$\overline{\nu_{22}}$ is the absorption peak position, expressed in wavenumber units (cm^{-1});

d_t is the diameter of SWCNTs, expressed in nanometer units (nm);

A_2 is 1 375 cm^{-1} and –1 475 cm^{-1} for (n – m) mod 3 = 1 and 2, respectively;

α is the chiral angle (°).

Errors using these formulae are low, less than 65 cm^{-1} in all cases, which is far below the spectral line widths of 150 cm^{-1} to 200 cm^{-1}[2][9][11].

NOTE 1 A_1 and A_2 are parameters to predict the experimental values based on the semi-empirical fit[2]. These values depend on the type of SWCNTs[2].

NOTE 2 Spectral peak positions are very sensitive to the solvent[14], surfactant coating[15] and filling state of SWCNTs[16][17].

NOTE 3 Recently, more comprehensive assignments for the optical transition energy for SWCNTs suspended in vacuum have been reported[13].

8.2 Determination of the chiral indices of the semi-conducting SWCNTs in a sample

The PL signals from (n, m) nanotubes are obtained by starting with emission spectra that have been corrected for the wavelength-dependent sensitivity of the detection system and the wavelength-dependent excitation intensity at the sample. For each species, the E_{11} emission intensity at its E_{22} excitation maximum shall be integrated across the spectral peaks. If there are overlapping emission features, the magnitudes of the separate components shall be obtained by simulating the experimental emission curve as a sum of peaks, each of which is a Voigt function with appropriate width and shape parameters.

Each experimental (n, m) PL signal, expressed as an area in the PL mapping, is the product of the relative mass concentration of the (n, m) SWCNT species multiplied by the PL cross-section for that (n, m) species. PL cross-sections are the product of E_{22} absorption cross-sections and PL quantum yields. Under the assumption that the absorption cross-section and PL quantum yields are fixed for each (n, m), the relative mass concentrations of (n, m) species can thus be deduced by dividing the experimental (n, m) signals by the corresponding PL cross-sections. The diameter distribution is obtained from the relative mass concentrations of each (n, m) SWCNT. Both these quantities are modified by extrinsic effects (e.g. doping) with the PL quantum yield being particularly variable. These must be kept in mind when determining (n, m) distributions based on PL intensities.

NOTE 1 Accurate values of the PL cross-sections for all (n, m) SWCNTs have not yet been determined. Experimental and theoretical results are available for some SWCNTs[8][18][19]. It is acceptable to show PL intensities rather than derived mass concentrations because information of the PL cross-section is limited in the literature.

NOTE 2 PL cross-sections are variable. Doping, damage and other effects can cause very large (orders of magnitude) changes to PL intensity.

9 Uncertainties

Currently, the NIR-PL characterization of SWCNTs is accompanied by the risk of uncertainties that come from:

a) mis-assigning a sideband to an (*n*, *m*) species;

b) bundles of SWCNTs contained in the sample;

c) double-wall carbon nanotubes contained in the sample;

NOTE The emission from double-wall carbon nanotubes is currently controversial[20].

d) absorption of PL by the suspending medium;

e) self-absorption of PL by SWCNTs;

f) up-conversion PL of SWCNTs[21];

g) dispersants and solvents that can alter PL intensities;

h) doping and defects of SWCNTs[22][23];

i) fluorescent impurities;

j) relationship between the SWCNT mass fraction, length, OD and PL intensity, which is still under investigation[24];

k) stability and homogeneity of dispersion;

l) pH of dispersion.

10 Test report

The test report shall contain the information required by ISO/IEC 17025 complemented by the following (see Annex A):

a) all the information necessary for sonication and ultracentrifugation processes;

b) the pH of dispersion;

c) the type of apparatus used;

d) the emission and the absorption peak positions of each (*n*, *m*) type of semi-conducting SWCNTs in the sample;

e) the integrated PL intensities of each (*n*, *m*) type of semi-conducting SWCNTs in the sample;

f) uncertainty discussion including any information about chemical/physical environment that could cause changes in PL intensities.

Annex A
(informative)

Case studies

A.1 General

The determination of the (*n*, *m*) types of semi-conducting SWCNTs in several SWCNT samples and their relative integrated PL intensities are derived based on PL analyses. The examined SWCNTs were produced by direct injection pyrolytic synthesis (DIPS) that was one of CVD methods[25] and the pulsed-laser vaporization (PLV) method[26]. Detailed experimental procedures are described for each production method of SWCNTs.

A.2 SWCNTs synthesized by the DIPS method

A.2.1 Sample preparation

As-grown DIPS-SWCNTs (about 1 mg) were dispersed in about 15 ml of D_2O containing 1 % (mass fraction) of SDBS using an ultrasonic homogenizer equipped with a titanium alloy tip (13 mm in diameter). A pulsed ultra-sound was applied (on: 1 s, off: 2 s) with a power of 200 W for 30 min. A 20 ml vial was used as a sample container. Each solution was then centrifuged at 127 600*g* for 2,5 h with a swing rotor and the supernatant was used.

A.2.2 PL measurements

The PL was measured with a spectrofluorometer equipped with a Xenon lamp and a NIR photomultiplier (Hamamatsu H9170-75[1)]) module (see Figure A.1). The bandpass of light throughput and the scan steps were 5 nm and 10 nm, respectively, where these parameters were applied to both excitation and emission.

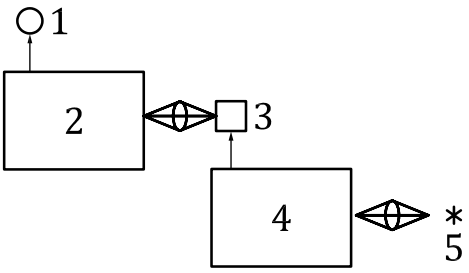

Key

1 photomultiplier
2 emission monochromator
3 sample cell
4 excitation monochromator
5 Xe lamp

Figure A.1 — Schematic illustration of experimental set-up

1) Hamamatsu H9170-75 is an example of a suitable product available commercially. This information is given for the convenience of users of this document and does not constitute an endorsement by ISO of this product.

Each PL peak in the two-dimensional PL excitation/emission map can be assigned to the individual chiral indices (*n, m*) according to the formulae in 8.1. For example, Figure A.2 shows a typical two-dimensional contour plot of the NIR-PL mappings of DIPS-SWCNTs/SDBS/D_2O. The PL peak positions measured experimentally are compared to those that have been empirically determined to correspond to a given (*n, m*)[11]. An identification of the (*n, m*) represented by a PL peak can be made when the difference between the experimental peak and the empirical peak positions is less than 65 cm^{-1} as shown in Figure A.2.

NOTE The empirically determined data of emission and absorption peaks for 220 (*n*, *m*) SWCNTs in an SDS micelle solution are listed in Reference [11].

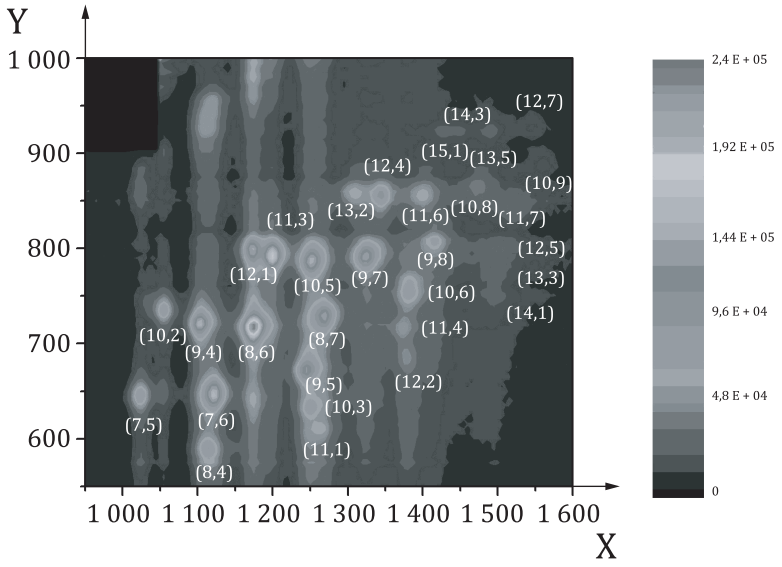

Key

X emission wavelength, in nm

Y excitation wavelength, in nm

Figure A.2 — Two-dimensional contour plot of the NIR-PL mappings of DIPS-SWCNTs/SDBS/D_2O[27]

A.2.3 Integrated PL intensities of each (*n*, *m*) type of semi-conducting SWCNTs

Figure A.3 shows the relative integrated PL intensities of each (*n*, *m*) type of semi-conducting SWCNTs in DIPS-SWCNTs (see Figure A.2) plotted as functions of diameter and chiral angle of the tubes, where the size of each circle denotes the relative integrated PL intensity. The obtained relative integrated PL intensities of all (*n*, *m*) types of semi-conducting SWCNTs are listed in Table A.1.

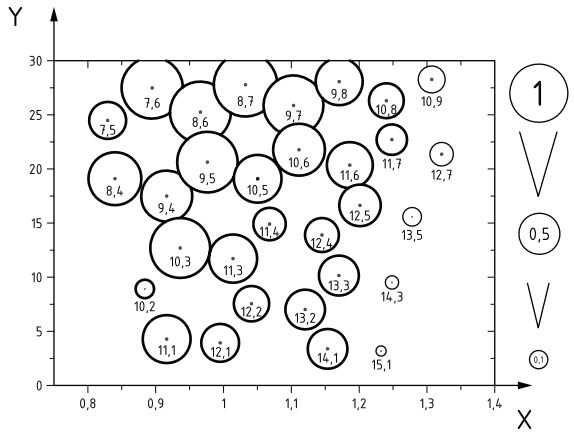

Key

X diameter, in nm

Y chiral angle, in deg

NOTE The areas of circles are proportional to the relative integrated PL intensities of the (*n*, *m*) type of semi-conducting SWCNTs.

Figure A.3 — Relative integrated PL intensities of each (*n*, *m*) type of semi-conducting SWCNTs in DIPS-SWCNTs/SDBS/D_2O[27]

Table A.1 — Relative integrated PL intensities of each (*n*, *m*) type of semi-conducting SWCNTs in DIPS-SWCNTs[27]

(*n*, *m*)	Diameter nm	Chiral angle degree	Emission peak position nm	Absorption peak position nm	Integrated PL intensity relative to the highest intensity species
(7, 5)	0,829	24,50	1 024	645	0,55 ± 0,03
(8, 4)	0,840	19,11	1 114	589	0,71 ± 0,04
(10, 2)	0,884	8,95	1 055	735	0,46 ± 0,03
(7, 6)	0,895	27,46	1 121	647	0,96 ± 0,08
(11, 1)	0,916	4,31	1 264	611	0,32 ± 0,03
(9, 4)	0,916	17,48	1 104	721	0,98 ± 0,08
(10, 3)	0,936	12,73	1 251	633	0,54 ± 0,06
(8, 6)	0,966	25,28	1 175	717	1,00 ± 0,06
(9, 5)	0,976	20,63	1 246	672	0,58 ± 0,07
(12, 1)	0,995	3,96	1 173	797	0,66 ± 0,06
(11, 3)	1,014	11,74	1 199	795	0,75 ± 0,05
(8, 7)	1,032	27,80	1 267	728	0,66 ± 0,05
(12, 2)	1,041	7,59	1 379	687	0,14 ± 0,02
(10, 5)	1,050	19,11	1 252	787	0,61 ± 0,03
(9, 7)	1,103	25,87	1 324	791	0,51 ± 0,03
(10, 6)	1,111	21,79	1 382	756	0,31 ± 0,02
(13, 2)	1,120	7,05	1 310	857	0,36 ± 0,05
(12, 4)	1,145	13,90	1 343	855	0,34 ± 0,04
(9, 8)	1,170	28,05	1 414	806	0,24 ± 0,03

NOTE The repeatability errors of integrated PL intensity relative to the highest intensity species are shown.

Table A.1 *(continued)*

(*n*, *m*)	**Diameter** nm	**Chiral angle** degree	**Emission peak position** nm	**Absorption peak position** nm	**Integrated PL intensity relative to the highest intensity species**
(11, 6)	1,186	20,36	1 399	855	0,30 ± 0,02
(12, 5)	1,201	16,63	1 501	797	0,15 ± 0,01
(15, 1)	1,232	3,20	1 427	923	0,022 ± 0,003
(10, 8)	1,240	26,33	1 474	865	0,15 ± 0,01
(14, 3)	1,248	9,52	1 448	923	0,026 ± 0,007
(13, 5)	1,278	15,61	1 489	923	0,052 ± 0,009
(10, 9)	1,307	28,26	1 558	886	0,072 ± 0,007
(12, 7)	1,321	21,36	1 544	927	0,064 ± 0,011
NOTE The repeatability errors of integrated PL intensity relative to the highest intensity species are shown.					

A.3 SWCNTs synthesized by the PLV method

A.3.1 Sample preparation

As-grown PLV-SWCNTs (about 1 mg) were dispersed in about 15 ml of D_2O containing 1 % (mass fraction) of SDBS using an ultrasonic homogenizer equipped with a titanium alloy tip (13 mm in diameter). A pulsed ultra-sound was applied (on: 1 s, off: 2 s) with a power of 200 W for 30 min. A 20 ml vial was used as a sample container. Each solution was then centrifuged at 127 600*g* for 2,5 h with a swing rotor and the supernatant was used.

A.3.2 PL measurements

The PL was measured with a home-built PL measurement system based on the Fourier transform infrared (FTIR) spectrometer with titanium-sapphire laser excitations and InGaAs detector (Hamamatsu G7754-01[1)]) (see Figure A.4). Standard InGaAs detectors have a cutoff around 1 650 nm and are not suitable for this type of sample. An extended NIR-PL system should be used[10][16][20].

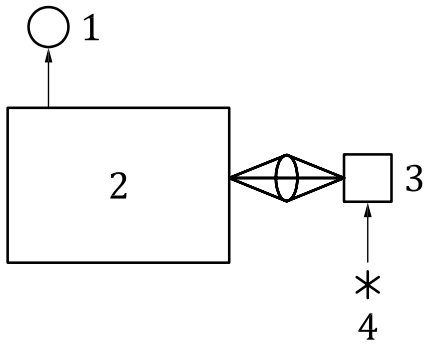

Key

1 detector
2 FTIR spectrometer
3 sample cell
4 titaniun-sapphire laser

Figure A.4 — Schematic illustration of experimental set-up

Each PL peak in the two-dimensional PL excitation/emission map can be assigned to the individual chiral indices (*n, m*) according to the formulae in 8.1. For example, Figure A.5 shows a typical two-dimensional contour plot of the NIR-PL mapping of PLV-SWCNTs/SDBS/D_2O. The PL peak positions measured experimentally are compared to those that have been empirically determined to correspond to a given (*n, m*)[11]. An identification of the (*n, m*) represented by a PL peak can be made when the difference between the experimental peak and the empirical peak positions is less than 65 cm^{-1} as shown in Figure A.5.

NOTE The data of emission and absorption peaks for 220 (*n*, *m*) SWCNTs in an SDS micelle solution are listed in Reference [11].

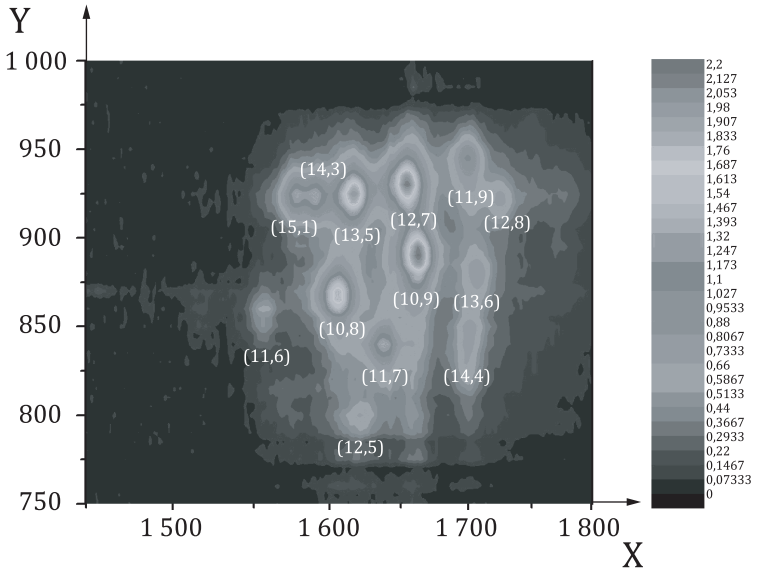

Key

X emission wavelength, in nm

Y excitation wavelength, in nm

NOTE The signal intensity is shown as colour bar (arbitrary unit).

Figure A.5 — Two-dimensional contour plot of the NIR-PL mappings of PLV-SWCNTs/SDBS/D_2O[20]

A.3.3 Integrated PL intensities of each (*n*, *m*) type of semi-conducting SWCNTs

Figure A.6 shows the relative integrated PL intensities of each (*n*, *m*) type of semi-conducting SWCNTs in PLV-SWCNTs (see Figure A.5) plotted as functions of diameter and chiral angle of the tubes, where the size of each circle denotes the relative integrated PL intensity. The obtained relative integrated PL intensities of all (*n*, *m*) types of semi-conducting SWCNTs are listed in Table A.2.

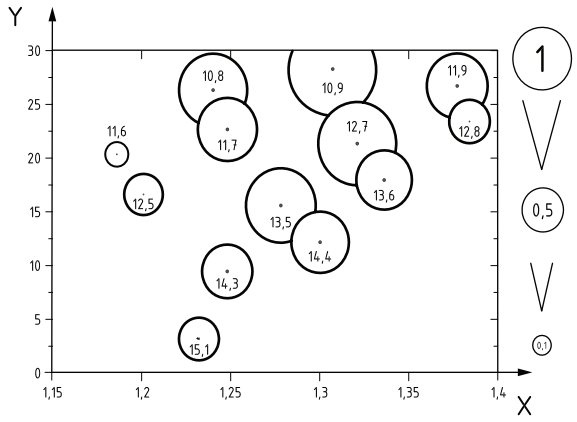

Key

X diameter, in nm

Y chiral angle, in deg

NOTE The areas of circles are proportional to the integrated PL intensities of the (*n, m*) type of semi-conducting SWCNTs.

Figure A.6 — Relative integrated PL intensities of each (*n*, *m*) type of semi-conducting SWCNTs in PLV-SWCNTs/SDBS/D_2O[20]

Table A.2 — Relative integrated PL intensities of each (*n*, *m*) type of semi-conducting SWCNTs in PLV-SWCNTs[20]

(*n*, *m*)	Diameter nm	Chiral angle degree	Emission peak position nm	Absorption peak position nm	Integrated PL intensity relative to the highest intensity species
(11, 6)	1,186	20,36	1 401	860	0,087 ± 0,004
(12, 5)	1,201	16,63	1 501	795	0,32 ± 0,02
(15, 1)	1,232	3,20	1 431	922	0,38 ± 0,03
(10, 8)	1,240	26,33	1 477	871	0,88 ± 0,02
(14, 3)	1,248	9,52	1 453	922	0,42 ± 0,06
(11, 7)	1,248	22,69	1 519	838	0,49 ± 0,02
(13, 5)	1,278	15,61	1 493	924	0,78 ± 0,04
(14, 4)	1,300	12,22	1 627	844	0,42 ± 0,05
(10, 9)	1,307	28,26	1 563	891	1,00 ± 0,03
(12, 7)	1,321	21,36	1 551	930	0,99 ± 0,08
(13, 6)	1,336	17,99	1 639	876	0,30 ± 0,02
(11, 9)	1,377	26,70	1 624	949	0,43 ± 0,02
(12, 8)	1,384	23,41	1 664	919	0,27 ± 0,03

NOTE The repeatability errors of integrated PL intensity relative to the highest intensity species are shown.

Bibliography

[1] Saito R., Dresselhaus G., Dresselhaus M.S. *Physical Properties of Carbon Nanotubes.* Imperial College Press, London. 1998. pp. 37–39. ISBN 1-86094-223-7

[2] Bachilo S.M., Strano M.S., Kittrell C., Hauge R.H., Smalley R.E., Weisman R.B. Structure-Assigned Optical Spectra of Single-Walled Carbon Nanotubes. *Science*. 2002, 298(5602), pp. 2361–2366

[3] Wang F., Dukovic G., Brus L.E., Heinz T.F. The Optical Resonances in Carbon Nanotubes Arise from Excitons. *Science*. 2005, 308(5723), pp. 838–841

[4] Nish A., Hwang J.-Y., Doig J., Nicholas R.J. Highly selective dispersion of single-walled carbon nanotubes using aromatic polymers. *Nature Nanotechnol.* 2007, 2, pp. 640–646

[5] Chen F., Wang B., Chen Y., Li L.-J. Toward the extraction of single species of single-walled carbon nanotubes using fluorene-based polymers. *Nano Lett.* 2007, 7(10), pp. 3013–3017

[6] Decker J.E., Hight Walker A.R., Bosnick K., Clifford C.A., Dai L., Fagan J., Hooker S., Jakubek Z.J., Kingston C., Makar J., Mansfield E., Postek M.T., Simard B., Sturgeon R., Wise S., Vladar A.E., Yang L., Zeisler R. Sample preparation protocols for realization of reproducible characterization of single-wall carbon nanotubes. *Metrologia*. 2009, 46(6), pp. 682

[7] Zheng M., Jagota A., Semke E.D., Diner B.A., McLean R.S., Lustig S.R., Richardson R.E., Tassi N.G. DNA-assisted dispersion and separation of carbon nanotubes. *Nat. Mater.* 2003, 2(5), pp. 338–342

[8] Kam N.W.S., O'Connell M., Wisdom J.A., Dai H. Carbon nanotubes as multifunctional biological transporters and near-infrared agents for selective cancer cell destruction, *Proc. Natl. Acad. Sci.* 2005, 102(33), pp. 11600–11605

[9] Weisman R.B. Fluorescence Spectroscopy of Single-Walled Carbon Nanotubes. In: Rotkin S.V., Subramoney S. (Eds.) *Applied Physics of Carbon Nanotubes: Fundamentals of Theory, Optics and Transport Devices*. Springer, Berlin. 2005, pp. 183–202

[10] Iakoubovskii K., Minami N., Kazaoui S., Ueno T., Miyata Y., Yanagi K., Kataura H., Ohshima S., Saito T., *J. Phys. Chem. B*. 2006, 110(35), pp. 17420–17424

[11] Weisman R.B., Bachilo S.M. Dependence of Optical Transition Energies on Structure for Single-Walled Carbon Nanotubes in Aqueous Suspension: An Empirical Kataura Plot. *Nano Letters.* 2003, 3(9), pp. 1235–1238

[12] Tsyboulski D.A., Rocha J.-D.R., Bachilo S.M., Cognet L., Weisman R.B. Structure-Dependent Fluorescence Efficiencies of Individual Single-Walled Carbon Nanotubes. *Nano Letters*. 2007, 7(10), pp. 3080–3085

[13] Liu K., Deslippe J., Xiao F., Capaz R.B., Hong X., Aloni S., Zettl A., Wang W., Bai X., Louie S.G., Wang E., Wang F. An atlas of carbon nanotube optical transitions. *Nat. Nanotechnol*. 2012, 7(5), pp. 325–329

[14] Ohno Y., Maruyama S., Mizutani T. Environmental Effects on Photoluminescence of Single-Walled Carbon Nanotubes. In: Marulanda J.M. (ed.) *Carbon Nanotubes*. IntechOpen, 2010. DOI: 10.5772/39421

[15] Okazaki T., Saito T., Matsuura K., Ohshima S., Yumura M., Iijima S. Photoluminescence Mapping of "As-Grown" Single-Walled Carbon Nanotubes: A Comparison with Micelle-Encapsulated Nanotube Solutions. *Nano Letters.* 2005, 5(12), pp. 2618–2623

[16] Okazaki T., Okubo S., Nakanishi T., Joung S.-K., Saito T., Otani M., Okada S., Bandow S., Iijima S. Optical Band Gap Modification of Single-Walled Carbon Nanotubes by Encapsulated Fullerenes. *J. Am. Chem. Soc.* 2008, 130 (12), pp. 4122–4128

[17] Cambré S., Wenseleers W. Separation and Diameter-Sorting of Empty (End-Capped) and Water-Filled (Open) Carbon Nanotubes by Density Gradient Ultracentrifugation. *Angew. Chem. Int. Ed.* 2011, 50(12), pp. 2764–2856

[18] Reich S., Thomsen C., Robertson J. Exciton resonances quench the photoluminescence of zigzag carbon nanotubes. *Phys. Rev. Lett.* 2005, 95(7), 077402

[19] Oyama Y., Saito R., Sato K., Jiang J., Samsonidze Ge.G., Grüneis A., Miyauchi Y., Maruyama S., Jorio A., Dresselhaus G., Dresselhaus M.S. Photoluminescence intensity of single-wall carbon nanotubes. *Carbon*. 2006, 44(5), pp. 873–879

[20] Okazaki T., Bandow S., Tamura G., Fujita Y., Iakoubovskii K., Kazaoui S., Minami N., Saito T., Suenaga K., Iijima S. Photoluminescence quenching in peapod-derived double-walled carbon nanotubes. *Phys. Rev. B*. 2006, 74, 153404–

[21] Akizuki N., Aota S., Mouri S., Matsuda K., Miyauchi Y. Efficient near-infrared up-conversion photoluminescence in carbon nanotubes. *Nat. Commun*. 2015, 6(8920). DOI: 10.1038/ncomms9920

[22] Ghosh S., Bachilo S.M., Simonette R.A., Beckingham K.M., Weisman R.B. Oxygen doping modifies near-infrared band gaps in fluorescent single-walled carbon nanotubes. *Science*. 2010, 330(6011), pp. 1656–1659

[23] Piao Y., Meany B., Powell L.R., Valley N., Kwon H., Schatz G.C., Wang Y. Brightening of carbon nanotube photoluminescence through the incorporation of sp3 defects. *Nat. Chem.* 2013, 5(10), pp. 840–845

[24] Fagan J.A., Simpson J.R., Bauer B.J., Lacerda S.H., Becker M.L., Chun J., Migler K.B., Walker A.R., Hobbie E.K. Length-dependent optical effects in single-wall carbon nanotubes. *J. Am. Chem. Soc.* 2007, 129(34), pp. 10607–10612

[25] Saito T., Ohshima S., Xu W.-C., Ago H., Yumura M., Iijima S. Size Control of Metal Nanoparticle Catalysts for the Gas-Phase Synthesis of Single-Walled Carbon Nanotubes. *J. Phys. Chem. B*. 2005, 109(21), pp. 10647– 10652

[26] Guo T., Nikolaev P., Thess A., Colbert D.T., Smalley R.E. Catalytic growth of single-walled manotubes by laser vaporization. *Chem. Phys. Lett.* 1995, 243(1–2), p. 49–54

[27] Okazaki T., Saito T., Matsuura K., Ohshima S., Yumura M., Oyama Y., Saito R., Iijima S. Photoluminescence and population analysis of single-walled carbon nanotubes produced by CVD and pulsed-laser vaporization methods. *Chem. Phys. Lett.* 2006, 420, p. 286–290

[28] Sansonettia J.E., Martin W.C. *Handbook of Basic Atomic Spectroscopic Data*. American Institute of Physics, 2005. DOI: 10.1063/1.1800011. Available from: https://www.nist.gov/pml/handbook-basic-atomic-spectroscopic-data

Bureau of Indian Standards

BIS is a statutory institution established under the *Bureau of Indian Standards Act*, 2016 to promote harmonious development of the activities of standardization, marking and quality certification of goods and attending to connected matters in the country.

Copyright

Review of Indian Standards

Amendments are issued to standards as the need arises on the basis of comments. Standards are also reviewed periodically; a standard along with amendments is reaffirmed when such review indicates that no changes are needed; if the review indicates that changes are needed, it is taken up for revision. Users of Indian Standards should ascertain that they are in possession of the latest amendments or edition by referring to the website-www.bis.gov.in or www.standardsbis.in

This Indian Standard has been developed from Doc No.: MTD 33 (20233).

Amendments Issued Since Publication

Amend No.	Date of Issue	Text Affected

BUREAU OF INDIAN STANDARDS

Headquarters:

Manak Bhavan, 9 Bahadur Shah Zafar Marg, New Delhi 110002
Telephones: 2323 0131, 2323 3375, 2323 9402 *Website*: www.bis.gov.in

Regional Offices:		*Telephones*
Central	: 601/A, Konnectus Tower -1, 6th Floor, DMRC Building, Bhavbhuti Marg, New Delhi 110002	2323 7617
Eastern	: 8th Floor, Plot No 7/7 & 7/8, CP Block, Sector V, Salt Lake, Kolkata, West Bengal 700091	2367 0012 2320 9474
Northern	: Plot No. 4-A, Sector 27-B, Madhya Marg, Chandigarh 160019	265 9930
Southern	: C.I.T. Campus, IV Cross Road, Taramani, Chennai 600113	2254 1442 2254 1216
Western	: Plot No. E-9, Road No.-8, MIDC, Andheri (East), Mumbai 400093	2821 8093

Branches : AHMEDABAD. BENGALURU. BHOPAL. BHUBANESHWAR. CHANDIGARH. CHENNAI. COIMBATORE. DEHRADUN. DELHI. FARIDABAD. GHAZIABAD. GUWAHATI. HIMACHAL PRADESH. HUBLI. HYDERABAD. JAIPUR. JAMMU & KASHMIR. JAMSHEDPUR. KOCHI. KOLKATA. LUCKNOW. MADURAI. MUMBAI. NAGPUR. NOIDA. PANIPAT. PATNA. PUNE. RAIPUR. RAJKOT. SURAT. VISAKHAPATNAM.

Published by BIS, New Delhi